Integrating UAVs and AI for Resilient Smart Energy Systems in Disaster

Muhtada Zuhair Ali [1], Jamshid Bagherzadeh[2] Parviz Rashidi-Khazaee[3*]

[1] Department of Electrical and Computer Engineering, Urmia University, Urmia, Iran
[2] Professor, Department of Electrical and Computer Engineering, Urmia University, Urmia, Iran
[3] Assistant Professor, Department of Information Technology and Computer Engineering, Urmia University of Technology, Urmia, Iran

*** Corresponding author email address**: p.rashidi@uut.ac.ir

Received: 2025-12-02 **Revised:** 2026-04-17 **Accepted:** 2026-04-25 **Initial Publish:** 2026-05-31 **Final Publish:** 2026-11-01

Abstract

Natural disasters pose serious challenges to smart grid infrastructure by simultaneously disrupting power and communication systems, leading to isolated microgrids or "islands". To support post-disaster recovery, this paper presents a multi-objective optimization framework for the efficient placement of unmanned aerial vehicle base stations (UAV-BSs) as mobile relay nodes connecting power sources (PSs) and static base stations (SBSs). The proposed method jointly optimizes geographical UAV-BS positions considering some conflicting objectives: minimizing the number of UAV-BSs and unserved PSs (NAPS), maximizing system throughput and energy efficiency. An enhanced Multi-Objective Reinforcement Learning (MORL) with clustering-based initialization is developed to improve convergence and solution diversity. Simulation results on the Simbench dataset confirm the effectiveness of the proposed approach in achieving robust, energy-efficient, and cost-effective UAV-BS deployment for smart grid restoration.

Keywords: *UAV-BS placement; MORL; multi-objective optimization; smart grid restoration; disaster management; energy efficiency; system throughput*

How to cite this article:

Zuhair Ali, M., Bagherzadeh, J., & Rashidi-Khazaee, P. (2026). Integrating UAVs and AI for Resilient Smart Energy Systems in Disaster. Management Strategies and Engineering Sciences, 8(6), 1-17.

1. Introduction

Ensuring the stability of power generation, transmission, and distribution is a primary goal of modern smart grids. However, increasing interconnectivity and exposure to extreme weather events have made these systems more vulnerable to large-scale disruptions. Natural disasters such as earthquakes, floods, and hurricanes can simultaneously damage both electrical and communication infrastructures [1]. This dual failure fragments the grid into isolated islands, making coordination and restoration challenging particularly in bottom-up recovery strategies, where independent microgrids must be synchronized before reintegration into the main grid [2].

Effective restoration relies on the information and communication technology (ICT) infrastructure that exchanges control and monitoring data between power sources (PSs) and supervisory nodes. When ICT components are damaged, some islands remain disconnected, delaying grid recovery [3]. In such cases, **unmanned aerial vehicle base stations (UAV-BSs)** can temporarily restore connectivity. Acting as mobile relays between PSs and static base stations (SBSs), UAV-BSs provide flexible and rapid communication recovery in disaster-affected areas where terrestrial repair is difficult [1].

A. Smart Grid Communication Components

The proposed model is based on a smart grid platform integrating ICT and power systems. Its main elements include:

1. **Power Source (PS):** Supplies energy and must remain connected to maintain network stability.
2. **Static Base Station (SBS):** Provides fixed communication links among PSs and with external networks.

3. **Mobile Base Station (MBS):** Includes vehicle- or UAV-mounted base stations for flexible communication support.
4. **Power Transmission Line (PTL):** Transports power between sources and base stations.

In the event of disasters, both PSs and BSs may fail, fragmenting the grid into functioning and non-functioning areas. In the figure 1, green zones (islands) represent operational clusters of BSs and PSs, while red zones indicate disconnected regions requiring recovery. Temporary **relay nodes (RNs)**—in this study implemented as UAV-BSs—can bridge communication gaps, reconnect isolated PSs, and restore overall network connectivity. Because UAV-BSs are more costly and energy-limited than fixed stations, their **optimal positioning** is essential for efficient and reliable operation.

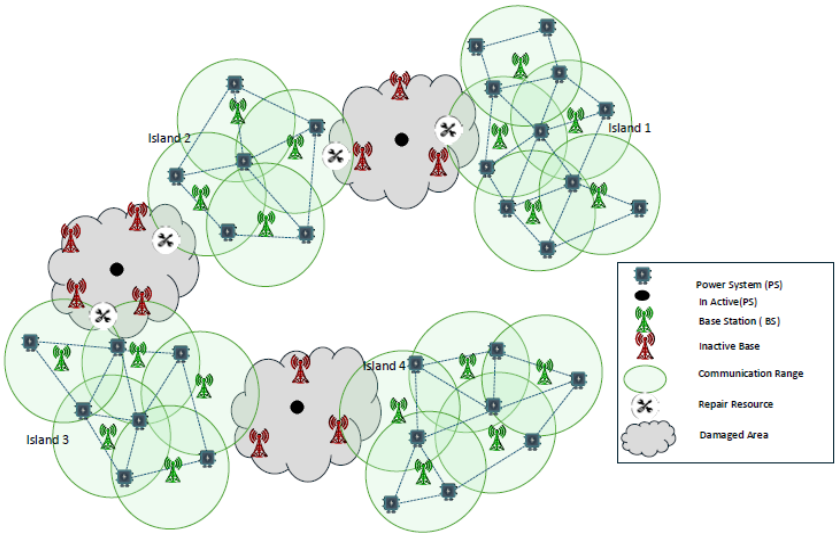

Figure 1. The smart grid network which turns into several islands after disaster

B. UAV-BS Features and Constraints

UAV-BSs, as part of **Low-Altitude Platforms (LAPs)** in **Non-Terrestrial Networks (NTNs)** [4], enable rapid deployment of communication backbones in emergency situations [5]. They offer several advantages: Quick and flexible deployment, Adjustable altitude for line-of-sight communication, and Cost-effective operation and adaptability to dynamic conditions. Nevertheless, UAV-BS operation is constrained by limited energy capacity, short flight duration, restricted communication range, and possible interference [7]. To ensure robustness, each UAV-BS should maintain reliable links with a minimum number of neighbors. Thus, their placement must balance connectivity, coverage, and energy consumption under these operational limits.

C. Problem Definition and Objectives

The UAV-BS deployment task can be formulated as a **multi-objective optimization problem** that considers several conflicting goals: minimize the number of UAV-BSs, minimize the number of unserved PSs, maximize system throughput, and maximize the energy efficiency. Balancing these objectives requires an algorithm capable of managing trade-offs among them. Existing studies have used heuristic and swarm-based methods such as Particle Swarm Optimization (PSO) [6].

To overcome these limitations, this paper proposes an **enhanced MORL** integrated with a **clustering-based initialization** mechanism. The proposed approach optimizes the geographical placement of UAV-BSs and PSs associations to BSs. This integration accelerates convergence, improves population diversity, and prevents premature stagnation. Extensive simulations on the **Simbench** benchmark dataset demonstrate that the proposed MORL framework achieves efficient, robust, and cost-effective UAV-BS deployment for post-disaster smart grid recovery.

By optimizing UAV placement across multiple objectives and incorporating clustering into MORL, the proposed method strengthens the resilience of smart grid communication networks, offering faster recovery, improved coverage, and higher energy efficiency in disaster conditions.

2. Related Works

The deployment of Unmanned Aerial Vehicle Base Stations (UAV-BSs) has emerged as a vital solution to restore connectivity during natural disasters and large-scale events. This section reviews existing studies on UAV-BS positioning, relay node placement, and communication frameworks, categorized by methodology and motivation.

A. Motivation and FSO-Assisted Drone Networks

In disaster scenarios or high-density environments such as stadiums, static base stations (SBSs) often fail to deliver adequate service. UAV-BSs can quickly reestablish coverage, compensating for damaged terrestrial infrastructure. However, their limited battery life and operational costs make energy-aware deployment essential.

Recent research introduced **Free Space Optics (FSO)**–assisted drone networks to improve resilience. In this architecture, Drone Base Stations (DBSs) connect mobile users via radio-frequency (RF) links and transmit backhaul data to macro base stations (MBSs) through high-capacity FSO channels [7]. The **RESCUE framework** jointly optimizes the 3D placement of DBSs, user assignments, and bandwidth distribution to maximize the number of users meeting target data rates [8].

B. Graph-Theoretical and Greedy Placement Strategies

Relay node (RN) deployment has also been approached through geometric and graph-based optimization.

- The **Connected Inter-Sectoral Topology (CIST)** algorithm models the service region as sectors and approximates a Steiner minimum tree to interconnect them using the fewest RNs [9].
- The **PSA-CIST** method extends this idea for smart grids by representing each island as a node and optimizing candidate RN positions within each [10].
- Other algorithms, such as **MST-1tRNP** and multi-stage heuristics, rely on minimum spanning trees or Steiner tree approximations. Although computationally efficient, these approaches often yield near-optimal rather than globally optimal results due to the NP-hard nature of the problem [10].

C. Distributed and Behavior-Aware UAV Deployment

Because individual UAVs have limited communication range, distributed algorithms have been proposed to enable self-organized global coverage.

- **Virtual Force (VF)** and **area-partitioning** approaches allow UAVs to adjust positions autonomously using local neighbor information [11].
- The **Coulomb–Voronoi Distributed (CVD)** algorithm applies virtual Coulomb forces and Voronoi diagrams for adaptive repositioning, enhancing coverage and reducing energy use [12].
- Hybrid methods integrate **Particle Swarm Optimization (PSO)** with behavior-based control, where PSO computes target positions and the controller guides UAVs while avoiding obstacles—forming real-time, multi-hop ad hoc networks in unknown terrains [13].

D. Optimization and Metaheuristic Techniques

Metaheuristic optimization has proven highly effective for UAV placement under complex, multi-objective conditions.

- Algorithms based on **PSO**, **Genetic Algorithms (GA)**, and other bio-inspired models jointly optimize UAV altitude, coverage, and energy efficiency [14].
- Variants like **chaotic PSO** (e.g., Tent-mapped initialization) improve exploration and prevent premature convergence [15].
- Two-stage PSO models for **drone swarm self-organizing networks** enhance throughput through collaborative beamforming and robust routing [16].
- **Hybrid PSO–Gray Wolf Optimization (PSOGWO)** approaches also demonstrate promise in multi-UAV coordination tasks, including search and rescue [17].

E. Machine Learning-Based Methods

Machine learning has been increasingly applied to UAV positioning problems due to its strong predictive and adaptive capabilities. A **self-healing neural model** combined with graph coloring has been proposed to determine UAV positions that maximize throughput and user association [18]. In [19], an energy-efficient deployment scheme minimizes total drone power consumption while ensuring user coverage. It first determines the required number of drones using improved *k*-means clustering, followed by optimal height and transmission power estimation. Similarly, **Hayajneh et al.** [20] grouped users into hotspots within a disaster zone and evaluated how drone count, location, and transmission power affect coverage probability and energy efficiency.

The **Aerostack framework** [21] incorporates deep learning into aerial robotics for perception, planning, and control across multiple abstraction layers. Moreover, **Deep Reinforcement Learning (DRL)** techniques such as **Deep Q-Network (DQN)**, **Deep Q-Learning (DQL)**, and **Liquid State Machine (LSM)** have been explored for grid communication problems, addressing access control, routing, and caching [22].

Other studies applied **reinforcement learning (RL)** to optimize UAV positioning for maximum user coverage under backhaul and radio constraints [23]. Hybrid frameworks combining **genetic algorithms** for global search and **hill-climbing** for local refinement have been proposed to enhance robustness and minimize redundancy in post-disaster communication [24].

3. Proposed Method

We address UAV-based base station (UAV-BS) deployment to restore connectivity in disaster-affected networks consisting of power stations (PSs) and base stations (BSs). Natural disasters can fragment the network into isolated islands, where intra-island BS communication remains functional but inter-island links are disrupted. PSs in disconnected regions lose service. UAV-BSs can simultaneously (i) provide coverage to uncovered PSs and (ii) reconnect SBSs. Both UAV-BSs and SBSs are constrained by maximum service range and the number of PSs they can support, determined by transmission power. Combined with throughput, coverage, and energy requirements, UAV-BS deployment constitutes a multi-objective optimization problem.

The aim is to determine UAV-BS geographical positions (x, y) that:

1. Minimize the number of UAV-BSs and isolated islands.
2. Maximize PS coverage and overall system throughput.
3. Maximize energy efficiency while satisfying PS rate requirements.

All network elements within an island must remain connected, and each PS must be served by either an SBS or UAV-BS. Additional challenges include limited UAV availability, conflicting objectives, and a need for comprehensive performance metrics beyond prior works.

To solve this, we employ **MORL (Multi-Objective Reinforcement Learning)**, a widely used evolutionary algorithm for multi-objective optimization. NSGA-II is capable of producing a diverse set of **Pareto-optimal solutions**, allowing decision-makers to select trade-offs between competing objectives without reducing them to a single scalar.

A. MORL Overview

Multi-Objective Reinforcement Learning (MORL) is an extension of classical reinforcement learning (RL) that addresses decision-making problems involving multiple, often conflicting, objectives. MORL optimizes a vector-valued reward that captures different objectives simultaneously [25].

In a conventional RL setup, an agent interacts with an environment defined by a tuple (S, A, P, R, γ), where S represents the state space, A is the action space, P is the transition probability, R is the reward function, and γ is the discount factor. The goal is to find an optimal policy $\pi(a|s)$ that maximizes the expected cumulative return.

In MORL, the reward is represented as a vector [25]:

$r_t = [r_t{}^{(1)}, r_t{}^{(2)}, \ldots, r_t{}^{(n)}]$

where each $r_t{}^{(i)}$ corresponds to a different objective. Consequently, the return becomes multi-dimensional:

$$G_t = \sum_{k=0}^{\infty} \Sigma \ (\gamma^k * r_{t+k+1}) \quad (1)$$

the symbol k is an index variable representing the time step offset from the current time t. At time t, $k = 0$ is the immediate reward (r_{t+1}), while $k = 1$ is the next reward (r_{t+2}). The **discount factor** $\gamma \in [0,1]$ ensures that **future rewards are worth less** than immediate ones, modeling uncertainty and time preference. In other words, γ^k reduces the importance of rewards that come k steps lat er. The return G_t is the **total discounted sum of future reward vectors** starting from time t, where each reward r_{t+k+1} is **weighted by how far into the future** it occurs.

The primary goal is to find policies that achieve desirable trade-offs among objectives of UAV-BSs positioning, often expressed as Pareto-optimal solutions. Pareto- Based MORL optimize a set of policies that approximate the Pareto front. A policy π_1 dominates another π_2 if and only if it performs at least as well in all objectives and strictly better in at least one. Typical Pareto-based algorithms include:

- Pareto Q-learning: maintains Q-values for each objective and selects non-dominated actions
- Policy gradient methods with Pareto ranking
- Hybrid evolutionary MORL (e.g., combining NSGA-II with RL)

B. Proposed MORL for UAV-BSs Placement

The proposed Hybrid MORL algorithm integrates reinforcement learning–based policy refinement into the traditional NSGA-II evolutionary framework for solving the considered problem. Also, machine learning method is used in initialization part of the proposed MORL. The algorithm proceeds through the following steps:

1. **Initialization:** One of the most important innovations of the proposed algorithm compared to conventional MORL is the initialization step. Generate an initial population of candidate UAV-BS placement and association decisions. The initial individuals are produced using a combination of greedy-based heuristics and random generation within the defined environmental boundaries to ensure both quality and diversity in the search space. In this step, some clustering methods including K-Means, DBSCAN, Agglomerative Hierarchical Clustering, Gaussian Mixture Models and Mean Shift are used to generate the candidate UAV-BS placement. Then, nearest UAV-BS is selected as association decision. Finally, in this step, initialize an empty external archive to store non-dominated solutions.
2. **Evaluation:** For each candidate solution, simulate the UAV-BS deployment environment and compute the objective function values. The key objectives include:
    - **Maximizing network coverage** (minimizing the number of uncovered PSs),
    - **Maximizing system throughput** (sum data rate of all connected PSs),
    - **Maximizing total energy efficiency**, and
    - **Minimizing the number of deployed UAV-BSs and islands**.

The evaluation also verifies system constraints, such as power and capacity limits, to ensure feasibility.

3. **Non-dominated Sorting:** Classify all solutions into several Pareto fronts based on dominance relationships. Solutions in the first front are non-dominated with respect to all objectives, while those in subsequent fronts are dominated by solutions in higher fronts.
4. **Crowding Distance Assignment:** Compute the crowding distance for each solution within a front to estimate the density of neighboring solutions. This helps preserve diversity along the Pareto front and prevents premature convergence.
5. **Selection:** Apply binary tournament selection based on the Pareto rank and crowding distance. Parents with lower rank (better front) and higher crowding distance (more diverse) are preferred for reproduction
6. **Crossover & Mutation:** Generate offspring by applying **Simulated Binary Crossover (SBX)** and **Polynomial Mutation** operators on the parent solutions. These genetic operators allow exploration of new UAV-BS configurations and improve convergence toward the optimal Pareto front.
7. **Local Reinforcement Learning Fine-Tuning (Hybridization Step):** For each newly generated offspring, perform a limited number of reinforcement learning (RL) updates to improve the policy parameters corresponding to UAV-BS placement and user association decisions. The RL component refines solutions by interacting with the environment and learning from feedback (e.g., signal-to-interface plus noise ratio, system throughput, energy efficiency).

This hybridization enhances local search capability and accelerates convergence toward high-quality solutions.

8. **Population Update:** Combine the parent and offspring populations and reapply non-dominated sorting and crowding distance calculations. Select the top N solutions (according to rank and diversity) to form the next generation.
9. **Pareto Archive Maintenance:** Update the external Pareto archive by adding newly non-dominated solutions and removing dominated ones. The archive maintains the best trade-offs among multiple objectives across all generation
10. **Termination:** Repeat the evaluation–selection–update process until a stopping criterion, which is maximum number of generations, is met. The final Pareto archive represents the set of optimal trade-offs among the number of selected UAV-BSs, coverage, throughput, energy efficiency.

The pseudo code of the proposed MORL algorithm is shown in the Fig. 2.

Inputs:
- Env: simulation environment for UAV-BS, PSs, BSs, channel / path-loss model
- N_pop: population size (number of candidate policies)
- N_gen: number of evolutionary generations
- eval_episodes: episodes per policy evaluation
- RL_steps: local RL update steps per offspring

Outputs:
- ParetoArchive: set of non-dominated policies (policy parameters and objective vectors)

Main:
1. Initialize population $P = \{\theta_1, \theta_2, \ldots, \theta_{N\_pop}\}$ (each θ is policy parameters including Place UAV-BSs (x, y, z coordinates), Assign PSs to BSs (association decision))
2. Initialize ParetoArchive $= \emptyset$
3. For gen = 1 to N_gen:
   # --- Evaluation Phase ---
   For each individual θ in P:
      load policy π = load_params(θ)
      feasible_count = 0
      For ep = 1 to eval_episodes:
         run one episode using π in Env, collect per-timestep multi-objective rewards
         At end of episode compute per-PS metrics:
          For each PS_u assigned to BS_v
             compute $PL_{PS_u}^{BS_v}$, $SINR_{PS_u}^{BS_v}$, bit-rate $B_{PS_u}^{BS_v}$, required power $P_{PS_u}^{BS_v}$, data transmission Capacity $SNR_{PS_u}^{BS_v}$
             compute data capacity C_u , energy efficiency $EE_{PS_u}^{BS_v}$
          Aggregate:
             System_throughput_episode = sum $B_{PS_u}^{BS_v}$ over all PSs
             total_capacity_episode = sum C_u
             total_power_episode = sum $P_{PS_u}^{BS_v}$
             total_EE_episode = total_capacity_episode / total_power_episode
          Check BS capacity limits: for each BS_v, ensure $sum\_received\_rates \leq T_x P_{B2P}$
          If constraint violated: mark episode infeasible feasibility_flag = false
          objectives_sum += [throughput_episode, total_EE_episode, total_capacity_episode]
          average_objectives = objectives_sum / eval_episodes
          apply penalty to average_objectives if feasibility_flag = false
          store θ.objectives = average_objectives

   # Create offspring:
   Offspring = []
   While len(Offspring) < N_pop:
      p1, p2 = tournament_select(P) # using Pareto rank + crowding
      c1_params, c2_params = crossover(p1.params, p2.params)
      c1_params = mutate(c1_params); c2_params = mutate(c2_params)
      Offspring.append(c1_params); Offspring.append(c2_params)
   # Truncate Offspring to N_pop if needed

   # --- Local RL Fine-Tuning on Offspring (exploitation) ---
   For each child_params in Offspring:
      policy = load_params(child_params)
      RL_fine_tune(policy, RL_steps) # small number of gradient updates (PPO/AC)
      child_params = flatten_params(policy)
      Reevaluate child_params as in Evaluation Phase to update objectives
      store child.objectives, child.feasible

   # --- Environmental Selection (form next generation) ---
   Pool = P ∪ Offspring
   P = NSGA2_selection(Pool) # keep N_pop individuals by rank+crowding

Figure 2. The pseudo code of the proposed MORL algorithm to select the UAV-BSs coordinates and PSs association

C. Problem Setup

The **Realistic Environment** is selected to evaluate the proposed algorithm. Geographical boundaries are defined by $(X_{low}, X_{up}, Y_{low}, Y_{up})$, with additional parameters summarized which shown in Table I [14]. Each PS has a unique ID, coordinates (x, y, h), and assigned BS. Each BS is described by an ID, location, transmission parameters, assigned PS count, and type which can be SBS or UAV-BS. PSs within SBS coverage are assigned directly. PSs are associated to one SBS that, in addition to the shortest distance, can support it given its capacity and limitations. Uncovered PSs are candidates for UAV-BS service. According to disaster-stricken network, which are defined for the problem, some PSs are out of services. Therefore, there is a need to use UAV-BSs to cover the environment and establish communication between BSs that have lost communication.

Table 1. The simulated parameters for UAV-BSs placement in disaster area

Parameter	Description	value
$SBS_{altitude}$	Altitude of static base stations	200 (m)
T_xR_{B2B}	Transmission range for BS to BS communication	280 (m)
T_xR_{B2P}	Transmission range for BS to PS communication	255 (m)
T_xP_{B2B}	Transmission power for BS to BS communication	150 (dB)
T_xP_{B2P}	Transmission power for BS to PS communication	140 (dB)
$ReciPow_{PS}^{min}$	Minimum allowed receiving power for PS	60 (w)
$ReciPow_{PS}^{min}$	Minimum allowed receiving power for BS	55 (w)
$DataRate_{PS}^{Threshold}$	Minimum data rate for PSs	0.2 (Mbps)
$MaxAssPSs$	Maximum number of PSs which can assign to one BS	12
$AnnGain_{BS}$	Antenna gain for the BS	60 (dB)
$AnnGain_{PS}$	Antenna gain for the PS	0 (dB)
$Bandwidth$	The total bandwidth	20 (MHz)
$NoisePower$	The value of noise power in the environment	4.7 (dBw)
$SysLoss$	Total system losses	2 (dB)
$AWGN$	Additive white gaussian noise	-174 (dBm/Hz)
$Freq_{B2B}$	Frequency between BS to BS	2.4 (GHz)
$Freq_{A2G}$	Carrier frequency of air to ground	2 (GHz)

D. UAV-BS Deployment

UAV-BSs are deployed incrementally to restore connectivity and coverage. MORL determines optimal 3D positions (x, y, h) and PSs association decision by balancing multiple objectives:

1. **Connectivity:** All BSs including SBSs and UAV-BSs form a single connected network.
2. **Coverage:** Ensure all PSs are served.
3. **Constraints:** UAV-BS, BS and PS limitations,
4. **Optimization goals:** energy efficiency, and system throughput.

E. Performance Metrics of Proposed MORL Algorithm

Key metrics include:

- Number of islands remaining.
- Number of uncovered PSs.
- Total system throughput, computed via Shannon capacity using signal-to-interface plus noise ratio (SINR), bandwidth, and path loss.

The SINR of PS_u property to BS_v is measured by the following equation [28]:

$$SINR_{PS_u}^{BS_v} = \frac{T^{BS_v} * PL_{PS_u}^{BS_v}}{\sum_{BS_i \in BSs, i \neq v} T^{BS_i} * PL_{PS_u}^{BS_i} + \gamma_0} \quad (2)$$

Where T^{BS_v} and $PL_{PS_u}^{BS_v}$ are the instantaneous transmission power of the BS_v sub channel and the path loss between PS_u and BS_v, respectively. In addition, γ_0 is the incremental Gaussian white noise (AWGN). Also, the Shannon theory is used to determine the bit rates of PS_u connected to BS_v. The considered equation is [26]:

$$B_{PS_u}^{BS_v} = \frac{N * W * log_2^{(1+SINR_{PS_u}^{BS_v})}}{\sum_{PS_u \in PSs} I_{PS_u}^{BS_v}} \quad (3)$$

where $I_{PS_u}^{BS_v}$ is one if PS_u is assigned to BS_v. Finally, the system throughput is calculated as sum of the bit rates of all PSs.

- Energy efficiency, measured as transmitted bits per unit of power. The following equations have been calculated to measure the energy efficiency.

$$P_{PS_u}^{BS_v} = \left(2^{R_{PS_u}^{BS_v}/B_{PS_u}^{BS_v}} - 1\right) PL_{PS_u}^{BS_v} * \sigma^2 \quad (4)$$

$$SP_{PS_u}^{BS_v} = P_{PS_u}^{BS_v} + AnnGain_{BS_v} - PL_{PS_u}^{BS_v} + AnnGain_{PS_u} - SysLoss \quad (5)$$

$$SNR_{PS_u}^{BS_v} = \frac{signal\ power}{noise\ power} = \frac{SP_{PS_u}^{BS_v}}{NP} \quad (6)$$

$$C_u = Blog_2^{(1+SNR_{PS_u}^{BS_v})} \quad (7)$$

$$EE_{total} = \frac{\sum_{u \epsilon PSs} C_u}{\sum_{u \epsilon PSs} P_{PS_u}^{BS_v}} \quad (8)$$

where $R_{PS_u}^{BS_v}$ is the received data rate corresponding to PS_u of BS_v. The other parameter to measures the power consumption of BS_v for communication with PS_u ($P_{PS_u}^{BS_v}$) is σ^2 (the power of the Gaussian noise with uniform and independent distribution). $AnnGain_{BS_v}$ ‘$AnnGain_{PS_u}$ and $SysLoss$ are the antenna gain for BS, the antenna gains for PS and the total system loss, respectively. The other two parameters are $SNR_{PS_u}^{BS_v}$ and C_u which are signal-to-noise ratio and data capacity between BS_v and PS_u, respectively.

F. Algorithm Workflow

1. Initialize environment, PS, and BS parameters and limitations.
2. Compute distance matrix that specifies the distance between BSs and PSs.
3. Assign PSs to SBSs based on distance matrix and the defined constrained; identify uncovered PSs.
4. Incrementally deploy UAV-BSs; MORL determines their 3D positions and association decisions.
5. Evaluate performance metrics: number of islands, uncovered PSs, system throughput, and energy efficiency.

This framework ensures efficient restoration of connectivity in disaster-stricken networks while optimizing multiple objectives simultaneously, providing a set of Pareto-optimal UAV-BS placements for flexible decision-making.

4. Configuration of Proposed MORL UAV-BS Placement Algorithm

The algorithm is composed of four main phases:

1. Parameter Initialization

Initially, some evolutionary algorithm and reinforcement learning parameters are defined as follow:

- **Population size:** 150 individuals
- **Number of Generations:** 500
- **SBX Crossover probability:** 0.9
- **Polynomial Mutation probability:** 0.1
- **Distribution indexes:** η_c = 20 (crossover), η_m = 20 (mutation)
- **External archive size:** 50 non-dominated solutions
- **Evaluation Episodes per Offspring (eval-episode):** 5
- **RL Learning Rate (α):** 0.01
- **Discount Factor (γ):** 0.99
- **Number of RL Gradient/Value Updates per Offspring:** 5
- **Batch size:** 64

In addition, some UAV deployment system parameters, which are define in Table I, include:

- Number of PSs and SBSs.
- **Subchannel parameters**:
  - Bandwidth per channel W
  - Number of subchannels N
- UAV-BS movement limits (min/max altitude).
- Transmission power of SBS/UAV-BS: T^{SBS}, T^{UAV-BS}
- Channel noise σ^2
- AWGN increment γ_0

The recommended parameter settings follow the most commonly reported values in the literature on multi-objective UAV deployment, NSGA-II optimization, and hybrid evolutionary–reinforcement learning frameworks. These parameters strike a balance between optimization efficiency and solution accuracy.

Each candidate solution encodes the **3D coordinates (x, y, h)** of UAV-BSs and the **association decision** for the PSs. The feasible **x, y** ranges is selected of the dataset. Also, the feasible altitude range is set between **50 m and 120 m** for urban environments. The characteristics of BSs and PSs are extracted from the **Simbench dataset** to maintain realistic spatial configurations.

2. Hybrid Population Initialization

Traditional random initialization may lead to poor population diversity. To improve convergence and exploration balance, initial individuals are generated using a **hybrid strategy**. The 3D coordinates are initialized by following two methods:

- **Clustering-based seeding:** positions derived from K-Means, DBSCAN, Fuzzy C-Means (FCM), and K-Medoids algorithms.
- **Random sampling:** used to fill the remaining population slots to ensure adequate diversity.

This approach ensures that individuals represent both **promising clusters** and **unexplored regions** of the search space.

Each individual, in addition to containing the position of the UAV-BSs, also contains the status of the assignment of PSs to BSs. For this purpose, all BSs that can support a PS, based on the distances and constraints, are placed in a list. Then, using a random method, one member of the list is selected for the PS.

3. Optimization Process

After the objective function evaluation, in each generation, the hybrid Evolutionary–RL optimization executes the following steps:

1. **Non-dominated sorting** of the current population.
2. **Crowding distance assignment** to maintain diversity among Pareto-optimal candidates.
3. **Binary tournament selection simulated binary crossover (SBX), and polynomial mutation** operations to generate offspring.
4. **Evaluation of individuals** based on multi-objective metrics, including network connectivity, number of uncovered PSs, energy efficiency, and throughput.
5. **RL-Based Local Refinement (The Hybrid Step):** Each offspring undergoes **policy-driven improvement** with 3 steps as follow:
    - **Initialize environment including UAV-BS geometry and PS association**
    - **In RL interaction,** for each episode, the **state** consist of UAV locations and PS positions is observed. Then, **take actions** which are moving the UAV-BS and reassign PS to different possible BS. Afterward, receive reward vector as **[**25**]**

$$\boldsymbol{r} = (\boldsymbol{r}_{ST}, \boldsymbol{r}_{EE}, \boldsymbol{r}_{Connectivity}, \boldsymbol{r}_{Coverage}) \quad (9)$$

Then, **Store transition** in reply buffer and update Q-network.

- **Apply learned adjustment:** offsprings have modified by RL with fine tuning UAV-BS positions and Improving PS associations

6. **Combination of parent and offspring populations**, followed by **elitist selection** of the best individuals for the next generation.

At the end of the optimization process, the **archive of non-dominated solutions** is sorted based on predefined objective priorities. The highest-ranked solution—representing the best trade-off among system throughput, energy efficiency, number of uncovered PSs, and inter-island connectivity—is selected as the **optimal UAV-BS deployment**.

5. Evaluation the Proposed MORL Model in Disaster Scenario

To verify the performance of the proposed UAV-BS placement strategy, we conducted simulation experiments in a disaster-affected scenario in which PSs and SBSs features are extracted from Simbench dataset [27]. The results from repeated executions of the algorithm confirmed its stability and effectiveness in re-establishing communication services.

A. Evaluation results on real data extracted of Simbench

A representative example is provided to better illustrate how the algorithm operates. Figure 3 presents the initial status of the network after the disruptive event. In this figure:

- PSs that maintain a connection to a BS are drawn as circle symbols
- SBS locations are presented using the standard base-station icon
- UAV-BSs are denoted with a UAV-shaped marker
- PSs without service are displayed as red cross-squares
- Different colors indicate which BS each PS is associated with

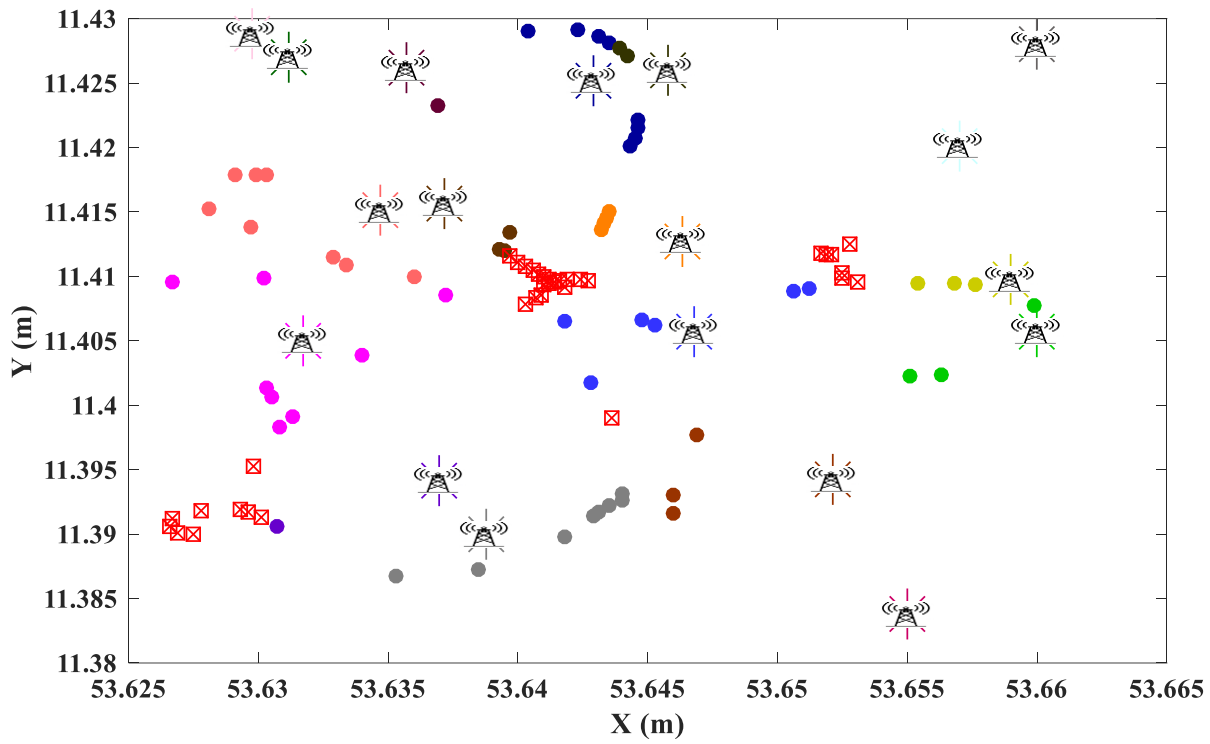

Figure 3. The initial status of the network after the disruptive event from Simbench

Due to the infrastructure damage, several SBSs were unable to function, causing 35 PSs to lose connectivity. The remaining active SBSs are separated into 6 distinct clusters, each forming a disconnected island. To make it easier to refer to BSs in the following, their geographical locations are introduced in Table II.

Table 2. The geographical location of static base station from one sample of Simbench dataset

BS id	longitude	latitude
1	53.6371661857949	11.4057536972748
2	53.6550127943866	11.4097536972748
3	53.6317489546179	11.4057536972748
4	53.6463192877302	11.4280000000000
5	53.6428864310562	11.4201415231307
6	53.6369891027391	11.4288039875136
7	53.6600000000000	11.3942136919934
8	53.6589891027391	11.3900000000000
9	53.6468014336777	11.4260021524272
10	53.6600000000000	11.4270505811915
11	53.6569891027391	11.4261613610700
12	53.6297419571506	11.4150939908510
13	53.6521206847920	11.4057536972748
14	53.6387603033120	11.4097536972748
15	53.6458014336777	11.4057536972748
16	53.6311826449690	11.4280000000000
17	53.6357274881303	11.4201415231307
18	53.6347069817339	11.4288039875136

The ids of BSs which placed in isolated islands are as follows:

- **First island:** 1, 3, 5, 12, 15, 16, 17, 18
- **Second island:** 2, 13
- **Third island:** 4, 9
- **Fourth island:** 6, 14
- **Fifth island:** 7, 8
- **Sixth island:** 10, 11

To recover the lost communication links, UAV-BSs are positioned through the proposed MORL-based deployment strategy. The algorithm determines both the horizontal locations and operating altitudes of the UAV-BSs and PSs associations by considering the surrounding environment and network performance criteria. Proper configuration of several algorithmic parameters is necessary for successful implementation. The selected parameter values were obtained through a grid-search procedure and aligned with commonly recommended configurations for MORL reported in earlier research.

The evaluation began with the deployment of a single UAV-BS in order to assess whether the defined objectives could be satisfied using the minimum number of aerial nodes. As illustrated in Fig. 4, the longitude, latitude and altitude which is selected for the UAV-BS are 53.6519, 11.4137 and 120m, respectively. this configuration resulted in 4 islands and 28 PSs remaining uncovered. The ids of BSs which placed in isolated islands are as follows:

- **First island:** 1, 3, 5, 12, 15, 16, 17, 18
- **Second island:** 2, 13
- **Third island:** 4, 7, 8, 9, 10, 11, 19
- **Fourth island:** 6, 14

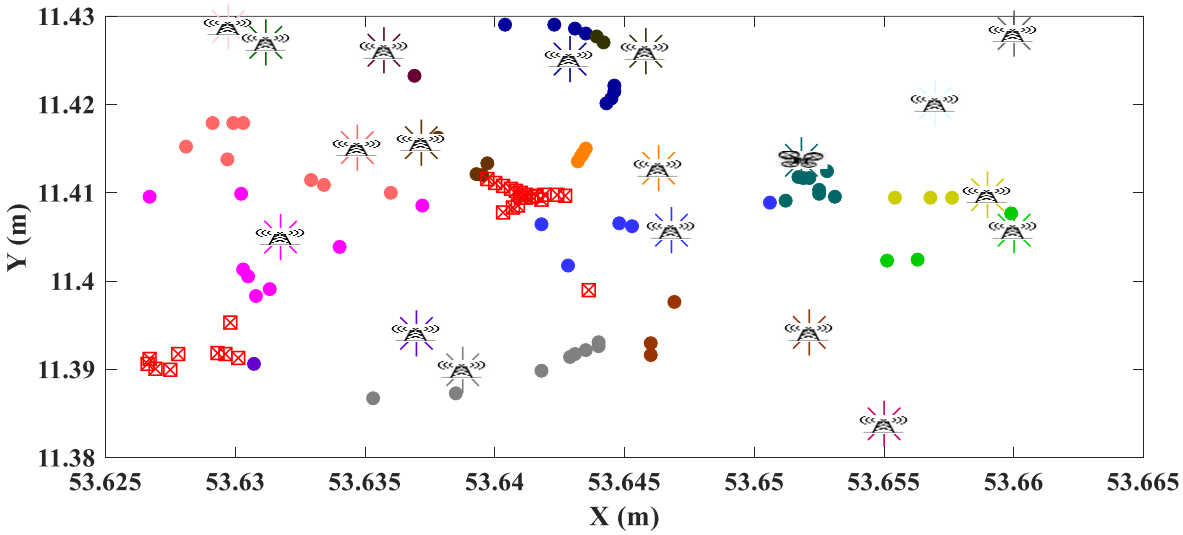

Figure 4. The status of the network after using one UAV-BS in environment

Because the problem formulation does not enforce a strict coverage guarantee, a single UAV-BS was insufficient to restore complete service across the network. As illustrated in Fig. 5, the number of UAV-BSs was increased to two, and the optimization was performed again. The longitude, latitude and altitude which are selected for two UAV-BS are as follows: $UAV-BS_x^1 = 53.6513, UAV-BS_y^1 = 11.4135, UAV-BS_h^1 = 120, UAV-BS_x^2 = 53.6400\,, UAV-BS_y^2 = 11.4050,\ UAV-BS_h^2 = 120$. In this case, the number of islands was reduced to 2 and the number of uncovered PSs dropped to 22, indicating a noticeable improvement. It is important to highlight that the primary objective is to minimize the number of islands, followed by reducing the number of uncovered PSs. The resulting UAV-BS placement successfully created additional communication links between SBSs, addressing the initial connectivity limitations. The ids of BSs in isolated islands are:

- **First island:** 1, 3, 4, 5, 6, 7, 8, 9, 10, 11, 12, 14, 15, 16, 17, 18
- **Second island:** 2, 13

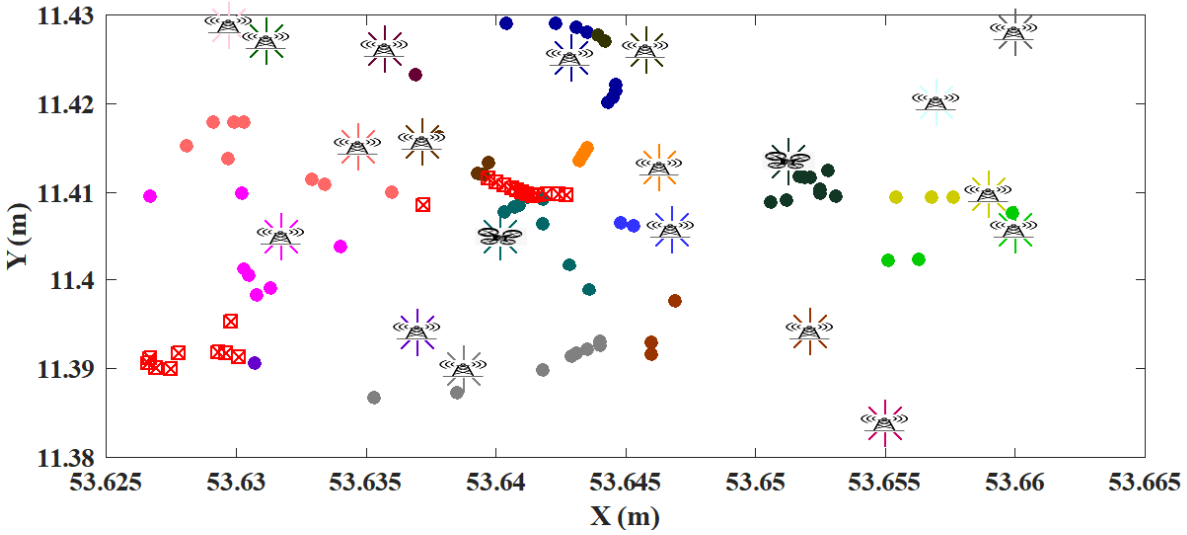

Figure 5. The status of the network after using two UAV-BSs in environment

Next, a third UAV-BS was introduced, and the updated network configuration is shown in Fig.6. This setup achieved the formation of a single island, while reducing the number of uncovered PSs to 9. In this state, the location of the UAV-BSs and their altitude are as follows:

- **UAV-BS 1:** x= 53.6426670368746, y= 11.3993239598744, h=108
- **UAV-BS 2:** x= 53.6409999782251, y= 11.4093997049084, h=118
- **UAV-BS 3:** x= 53.6520960799233, y= 11.4130422618970, h=120

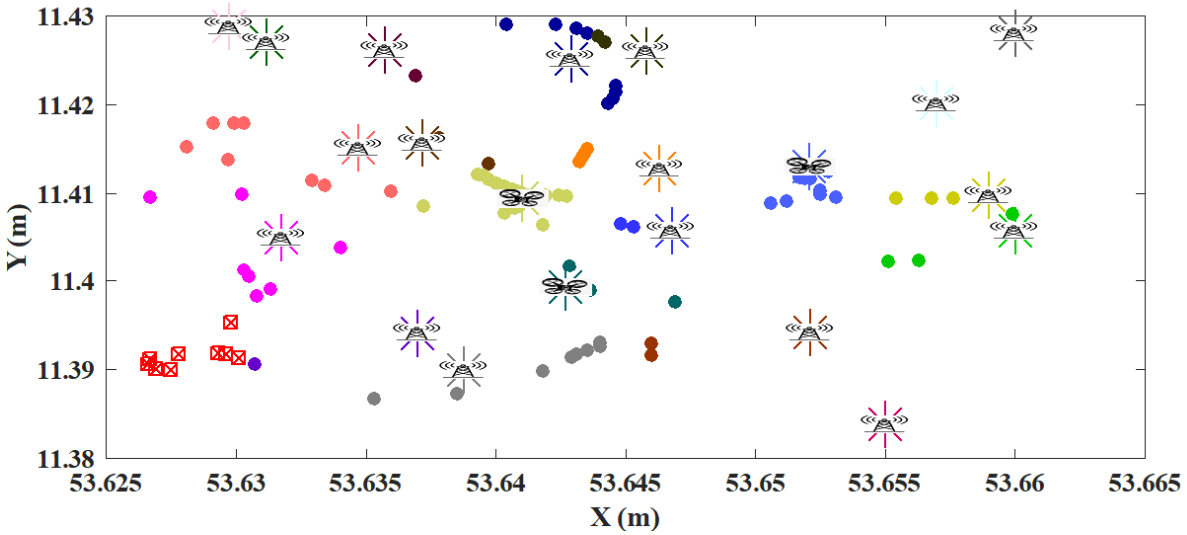

Figure 6. The status of the network after using three UAV-BSs in environment

To meet all constraints, a fourth UAV-BS was deployed, and the final results are presented in Fig.7. The corresponding UAV-BS coordinates and its altitudes are as follows:

- **UAV-BS 1:** x= 53.6283073591394, y= 11.3936228581266, h=120
- **UAV-BS 2:** x= 53.6518731501480, y= 11.4131521445278, h=120
- **UAV-BS 3:** x= 53.6428647548710, y= 11.3998521324587, h=108
- **UAV-BS 4:** x= 53.6412405619366, y= 11.4094198677112, h=119

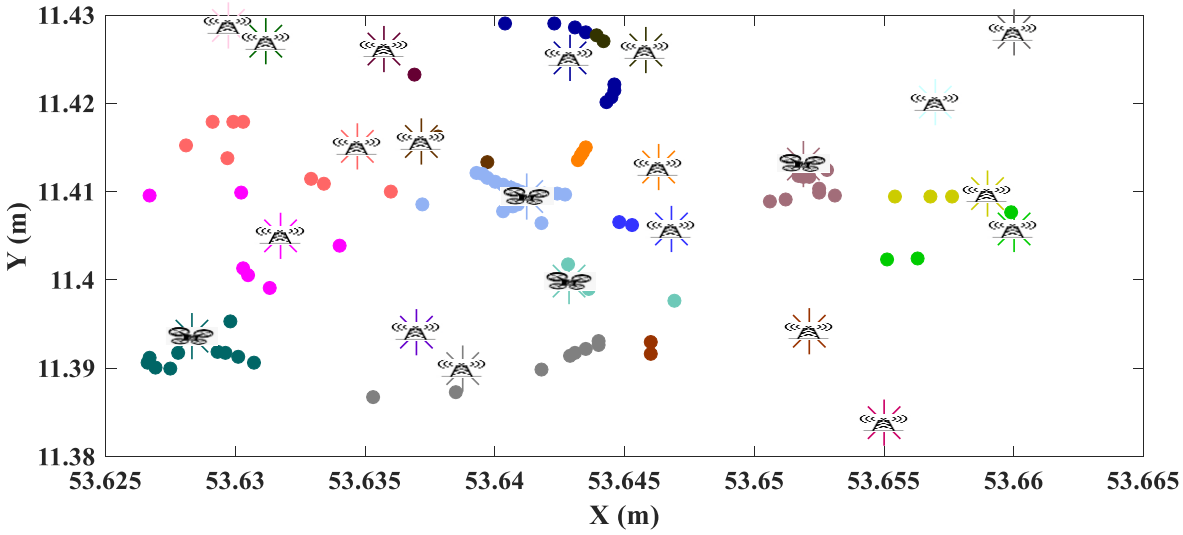

Figure 7. The status of the network after using four UAV-BSs in environment

At this stage of the deployment process, the proposed algorithm successfully fulfills all defined operational constraints. The optimized geographical positions and altitude of the UAV-BSs and PSs to BSs association are selected in accordance with the primary objectives of maximizing PS coverage and restoring complete network connectivity.

The MORL framework produces a diverse set of candidate solutions corresponding to the population size. The Pareto front reflects the best compromise among competing objectives. From this set, the final deployment configuration is chosen based on adherence to constraints and prioritized performance goals—namely, maximizing system throughput and total energy efficiency. Table III presents a comparative summary of the algorithm's performance across the four iterative deployment phases, where one UAV-BS is incrementally added at each step. As the number of UAV-BSs increases, the number of disconnected islands and uncovered PSs is progressively reduced, while the system throughput and energy efficiency consistently improve. When four UAV-BSs are deployed, all constraints are fully satisfied, and the performance indicators reach their most favorable values.

Table 3. Objective values obtained from the proposed algorithm based on the selected solutions for varying numbers of UAV-BSs

Number of UAV-BSs	# of Islands	# of Uncovered PSs	System Throughput	Energy Efficiency
1	4	28	42.9	20.1
2	2	22	45.12	22.13
3	1	9	46.08	24.6
4	1	0	48.76	27. 41

B. Evaluation results of clustering methods on real data extracted of Simbench

Next, the presented algorithm is compared with clustering algorithms. A widely used approach for identifying effective placement positions for UAV-BSs is the application of clustering methods. Although clustering offers a solid baseline configuration for UAV-BS deployment, additional optimization is required to fine-tune these initial points and move toward a more optimal arrangement. To determine whether optimization is required beyond the initial clustering stage, a comparative assessment was carried out. The analysis focused on evaluating if cluster-based UAV-BS locations alone can meet performance requirements, or whether further optimization yields noticeable improvements in coverage and overall system behavior. In earlier research [19], an enhanced version of the K-Means algorithm was applied to estimate the spatial positions of UAV-BSs, and the resulting deployment layout is shown in

Fig. 8. The clustering procedure relied on the spatial distribution of uncovered PSs, and because these points are dispersed unevenly throughout the area, the number of UAV-BSs produced by the clustering algorithm directly influenced the achievable coverage level.

- **Figure 8(a)** presents the scenario with a single UAV-BS. Because a large cluster of uncovered PSs is concentrated near the central region—while others remain dispersed—the clustering algorithm places the UAV-BS roughly at the center of the area. In this state, the number of islands and number of uncovered PSs are 6 and 30, respectively.
- **Figure 8(b)** shows the configuration obtained when two UAV-BSs are deployed. Since the clustering method prioritizes regions with the highest density of uncovered PSs, the second UAV-BS is positioned in the area containing the largest group of them. As a result, the algorithm does not account for reducing the number of disconnected islands. The number of islands remain 6, but the number of uncovered PSs reduces to 9.
- **Figure 8(c)** displays the outcome when three UAV-BSs are used. In this case, only one PS remains that is not covered. However, since the clustering method does not consider the number of islands, the space consists of 5 separate islands.
- **Figure 8(d,e)** illustrates the case with four UAV-BSs. Even with an additional UAV-BS, the clustering algorithm still fails to identify effective deployment positions that satisfy the required constraints and objectives. The number of uncovered PSs remains 1 and the number of islands reduces to 4. Considering the increase in the number of UAV-BSs to 5, none of the constraints of the problem are satisfied. In this case, the number of uncovered PSs and the number of islands are 2 and 3, respectively.

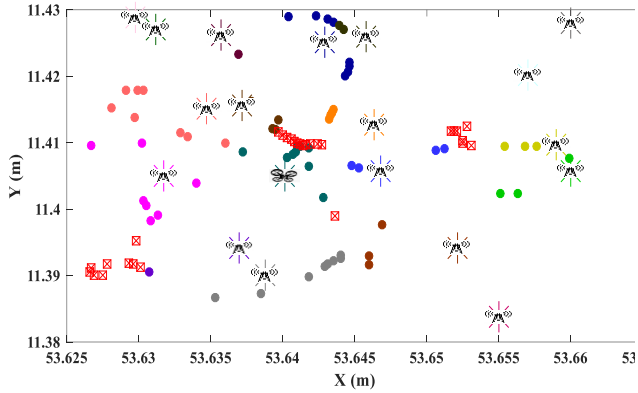

(a)

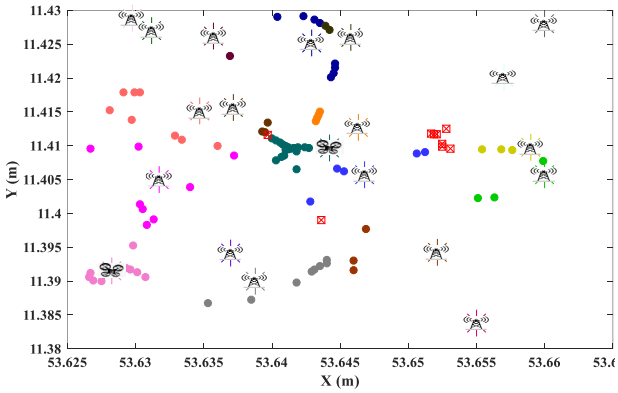

(b)

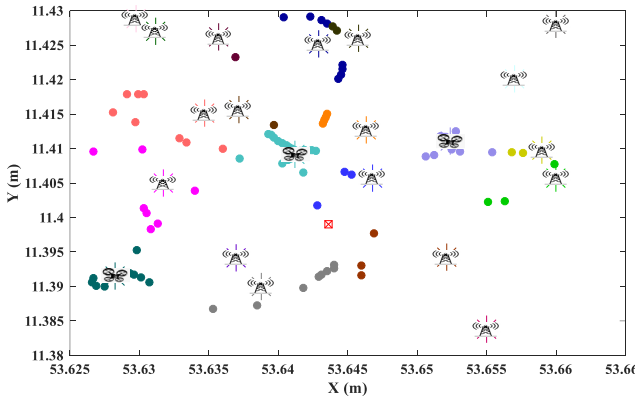

(c)

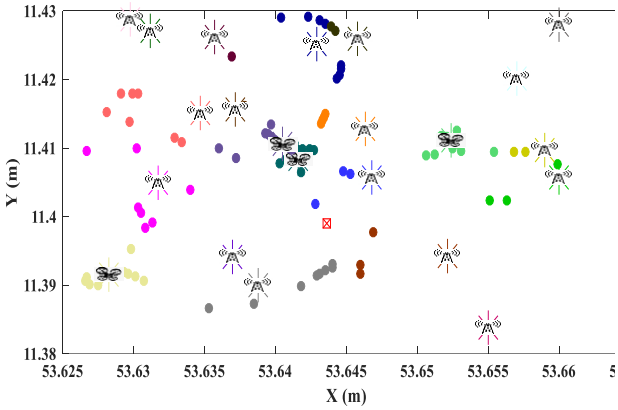

(d)

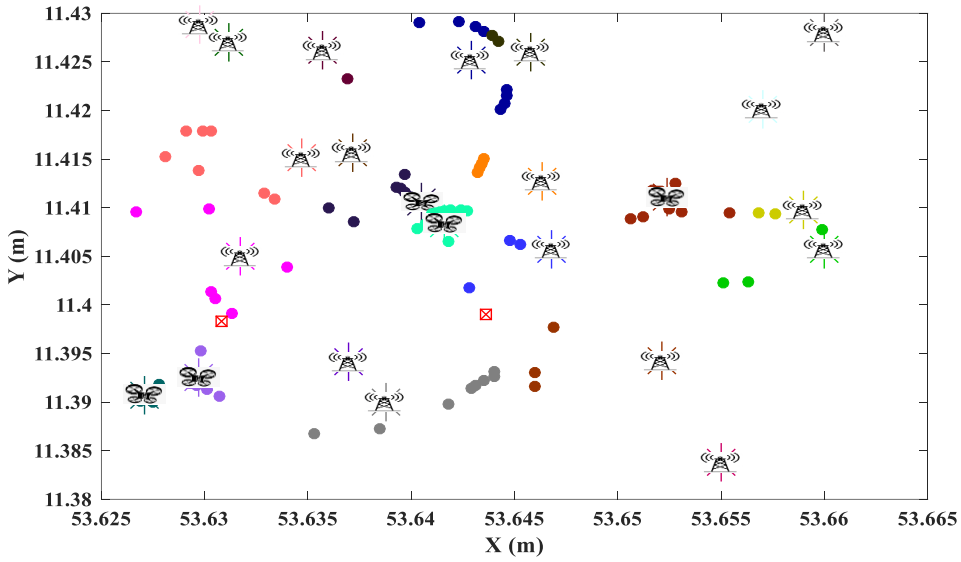

(e)

Figure 8. Senario Analysis

This finding underscores the weakness and inefficiency of clustering-only solutions when compared to the proposed MORL-based approach, which achieves full constraint satisfaction and higher system performance with fewer UAV-BSs.

Other clustering-based approaches were also tested; however, their performance showed no meaningful improvement over the optimized K-Means method. For this reason, only the results obtained from the optimized K-Means algorithm are reported. Overall, although clustering techniques can serve as a reasonable starting point for estimating initial UAV-BS locations, they are unable to capture the complex and multi-objective characteristics of the deployment problem. Consequently, clustering alone is insufficient for achieving high-quality solutions in this context.

C. Evaluation results of NSGA-II on real data extracted of Simbench

The following is a comparison of the proposed MORL method with NSGA-II. The results of a single run of the NSGA-II algorithm are shown in Table IV. It is worth noting that the algorithm does not have the ability to converge to exact solutions. Another problem with the NSGA-II algorithm is that each run can lead to a different result.

Table 4. Objective values obtained from the NSGA-II algorithm based on the selected solutions for varying numbers of UAV-BSs

Number of UAV-BSs	# of Islands	# of Uncovered PSs	System Throughput	Energy Efficiency
1	4	30	40.12	18.12
2	2	25	42.62	20.33
3	2	9	45.08	22.31
4	2	4	46.94	24. 31

6. Conclusion

This study introduces an integrated approach for restoring communication services in disaster-impacted smart grids by optimally positioning UAV-based base stations. The deployment task is modeled as a multi-objective optimization problem that incorporates critical constraints, including power usage, service coverage, and inter-BS connectivity. Within this framework, we propose a modified MORL algorithm that leverages clustering-driven initialization to generate high-quality search regions and effectively navigate the trade-offs between conflicting objectives. The method achieves a strong balance between

reducing the number of UAV-BSs, creating an island, increasing energy efficiency, and enhancing overall system throughput. The experimental evaluations, performed on both synthetic scenarios and benchmark real-world datasets, demonstrate the algorithm's reliability, efficiency, and adaptability under varying disaster conditions.

Looking ahead, further advancement may be achieved by incorporating mobile or trajectory-based UAV repositioning, integrating non-terrestrial networks such as satellite or HAPS systems, and developing real-time adaptive control mechanisms to strengthen communication resilience in large-scale and rapidly evolving disaster settings.

Authors' Contributions

Authors equally contributed to this article.

Acknowledgments

Authors thank all participants who participate in this study.

Declaration of Interest

The authors report no conflict of interest.

Funding

According to the authors, this article has no financial support.

Ethical Considerations

All procedures performed in this study were under the ethical standards.

References

[1] E. Casmin and E. Ever, "An analytical approach for modelling unmanned aerial vehicles and base station interaction for disaster recovery scenarios," *Wireless Networks,* vol. 30, no. 5, pp. 3299-3319, 2024. [Online]. Available: https://doi.org/10.1007/s11276-024-03734-0.

[2] X. J. Y. Wang, R. Tian, and H. Liu, "Coordinated Restoration of Microgrids and Generation Units for Resilience Enhancement of Urban Power Grids," *Journal of Electrical and Computer Engineering,* vol. 2025, no. 1, 2025. [Online]. Available: https://onlinelibrary.wiley.com/doi/abs/10.1155/jece/6375178.

[3] J. Zhong *et al.*, "Resilient microgrid formation considering communication interruptions," *Electronics Letters,* vol. 60, no. 14, p. e13275, 2024. [Online]. Available: https://ietresearch.onlinelibrary.wiley.com/doi/abs/10.1049/ell2.13275.

[4] J. Liu, Y. Shi, Z. M. Fadlullah, and N. Kato, "Space-air-ground integrated network: A survey," *IEEE Communications Surveys & Tutorials,* vol. 20, no. 4, pp. 2714-2741, 2018. [Online]. Available: https://doi.org/10.1109/COMST.2018.2841996.

[5] H. Hamid and G. R. Begh, "IRS assisted UAV communications for 6G networks: a systematic literature review," *Wireless Networks,* vol. 31, no. 1, pp. 779-807, 2025. [Online]. Available: https://doi.org/10.1007/s11276-024-03798-y.

[6] G. Ahmed, T. Sheltami, A. Mahmoud, and A. Yasar, "Energy-efficient UAVs coverage path planning approach," *Computer Modeling in Engineering & Sciences (CMES),* vol. 136, no. 3, pp. 3239-3263, 2023. [Online]. Available: https://doi.org/10.32604/cmes.2023.022860.

[7] A. Chaaban, J.-M. Morvan, and M.-S. Alouini, "Free-space optical communications: Capacity bounds, approximations, and a new sphere-packing perspective," *IEEE Transactions on communications,* vol. 64, no. 3, pp. 1176-1191, 2016. [Online]. Available: https://doi.org/10.1109/TCOMM.2016.2524569.

[8] N. Cvijetic, D. Qian, J. Yu, Y. K. Huang, and T. Wang, "100 Gb/s per-channel free-space optical transmission with coherent detection and MIMO processing," 2009: IEEE. [Online]. Available: https://ieeexplore.ieee.org/abstract/document/5287384/.

[9] F. Senel and M. Younis, "Optimized connectivity restoration in a partitioned wireless sensor network," 2011: IEEE.

[10] J. Zhong, C. Chen, Z. Bie, and M. Shahidehpour, "Strategic SDN-based microgrid formation for managing communication failures in distribution system restoration," *IEEE Transactions on Power Systems,* 2024. [Online]. Available: https://ieeexplore.ieee.org/abstract/document/10752412/.

[11] A. Trotta, M. Di Felice, F. Montori, K. R. Chowdhury, and L. Bononi, "Joint coverage, connectivity, and charging strategies for distributed UAV networks," *IEEE Transactions on Robotics,* vol. 34, no. 4, pp. 883-900, 2018. [Online]. Available: https://doi.org/10.1109/TRO.2018.2839087.

[12] X. Liu *et al.*, "Deployment of UAV-BSs for on-demand full communication coverage," *Ad Hoc Networks,* vol. 140, p. 103047, 2023. [Online]. Available: https://doi.org/10.1016/j.adhoc.2022.103047.

[13] N. D. T. Thuy, D. N. Bui, M. D. Phung, and H. P. Duy, "Deployment of UAVs for optimal multihop ad-hoc networks using particle swarm optimization and behavior-based control," 2022: IEEE. [Online]. Available: https://ieeexplore.ieee.org/abstract/document/9990164/.

[14] M. Sadeghi Ghahroudi, A. Shahrabi, S. M. Ghoreyshi, and F. A. Alfouzan, "Distributed node deployment algorithms in mobile wireless sensor networks: Survey and challenges," *ACM Transactions on Sensor Networks,* vol. 19, no. 4, pp. 1-26, 2023. [Online]. Available: https://doi.org/10.1145/3579034.

[15] S. Liu, W. Zhou, M. Qin, and X. Peng, "Tent-PSO-Based Unmanned Aerial Vehicle Path Planning for Cooperative Relay Networks in Dynamic User Environments," *Sensors,* vol. 25, no. 7, p. 2005, 2025. [Online]. Available: https://doi.org/10.3390/s25072005.

[16] X. Zheng *et al.*, "UAV swarm-enabled collaborative post-disaster communications in low altitude economy via a two-stage optimization approach," *arXiv preprint arXiv:2501.05742,* 2025. [Online]. Available: https://ieeexplore.ieee.org/abstract/document/11051254/.

[17] D. Han, H. Jiang, L. Wang, X. Zhu, Y. Chen, and Q. Yu, "Collaborative task allocation and optimization solution for

unmanned aerial vehicles in search and rescue," *Drones,* vol. 8, no. 4, p. 138, 2024. [Online]. Available: https://doi.org/10.3390/drones8040138.

[18] M. Kabiri, C. Cimarelli, H. Bavle, J. L. Sanchez-Lopez, and H. Voos, "A review of radio frequency based localisation for aerial and ground robots with 5g future perspectives," *Sensors,* vol. 23, no. 1, p. 188, 2022. [Online]. Available: https://doi.org/10.3390/s23010188.

[19] J. He *et al.*, "Machine learning based network planning in drone aided emergency communications," 2020: IEEE. [Online]. Available: https://ieeexplore.ieee.org/abstract/document/9129394/.

[20] A. M. Hayajneh, S. A. R. Zaidi, D. C. McLernon, M. Di Renzo, and M. Ghogho, "Performance analysis of UAV enabled disaster recovery networks: A stochastic geometric framework based on cluster processes," *IEEE Access,* vol. 6, pp. 26215-26230, 2018. [Online]. Available: https://doi.org/10.1109/ACCESS.2018.2835638.

[21] M. Fernandez-Cortizas, M. Molina, P. Arias-Perez, R. Perez-Segui, D. Perez-Saura, and P. Campoy, "Aerostack2: A software framework for developing multi-robot aerial systems," *arXiv preprint arXiv:2303.18237,* 2023. [Online]. Available: https://arxiv.org/abs/2303.18237.

[22] D. T. Hoang, N. Van Huynh, D. N. Nguyen, E. Hossain, and D. Niyato, *Deep Reinforcement Learning for Wireless Communications and Networking: Theory, Applications and Implementation*. John Wiley & Sons, 2023.

[23] A. Fotouhi, M. Ding, and M. Hassan, "Deep q-learning for two-hop communications of drone base stations," *Sensors,* vol. 21, no. 6, p. 1960, 2021. [Online]. Available: https://doi.org/10.3390/s21061960.

[24] Y. Angeles, V. K. Legaria-Santiago, H. Calvo, and A. Anzueto, "Dynamic Neural Network Optimization: A single agent neuroevolution algorithm based on hill climbing optimization for Neural Architecture Search," *International Journal of Combinatorial Optimization Problems & Informatics,* vol. 16, no. 1, 2025. [Online]. Available: https://search.ebscohost.com/login.aspx?direct=true&profile=ehost&scope=site&authtype=crawler&jrnl=20071558&AN=184481059&h=2GXT%2BZSV5NbHIzETv6xNZ7rZKuqS9GpMtJq1wrE97sAAzernSSn7DX4hKBT1NwpZqOuOZ7QcVUTsz3Dcg%2Fjz6Q%3D%3D&crl=c.

[25] C. Liu, X. Xu, and D. Hu, "Multiobjective reinforcement learning: A comprehensive overview," *IEEE Transactions on Systems, Man, and Cybernetics: Systems,* vol. 45, no. 3, pp. 385-398, 2014. [Online]. Available: https://doi.org/10.1109/TSMC.2014.2358639.

[26] S. Shukla, R. Thakur, and S. Agarwal, "Particle swarm optimization algorithms for altitude and transmit power adjustments in UAV-assisted cellular networks," 2021: IEEE.

[27] S. Meinecke *et al.*, "Simbench-a benchmark dataset of electric power systems to compare innovative solutions based on power flow analysis," *Energies,* vol. 13, no. 12, p. 3290, 2020. [Online]. Available: https://doi.org/10.3390/en13123290.